www.czasopisma.pan.pl PAN POLSKA AKADEMIA NAUK www.journals.pan.pl

Arch. Min. Sci. **67** (2022), 2, 317-332

Electronic version (in color) of this paper is available: http://mining.archives.pl

DOI: https://doi.org/10.24425/ams.2022.141461

DARIUSZ TOMASZEWSKI[1*], JACEK RAPIŃSKI[1], LECH STOLECKI[2], MICHAL ŚMIEJA[3]

SWITCHING EDGE DETECTOR AS A TOOL FOR SEISMIC EVENTS DETECTION BASED ON GNSS TIMESERIES

Contemporary mine exploitation requires information about the deposit itself and the impact of mining activities on the surrounding surface areas. In the past, this task was performed using classical seismic and geodetic measurements. Nowadays, the use of new technologies enables the determination of the necessary parameters in global coordinate systems. For this purpose, the relevant services create systems that integrate various methods of determining interesting quantities, e.g., seismometers / GNSS / PSInSAR. These systems allow detecting both terrain deformations and seismic events that occur as a result of exploitation.

Additionally, they enable determining the quantity parameters that characterise and influence these events. However, such systems are expensive and cannot be set up for all existing mines. Therefore, other solutions are being sought that will also allow for similar research. In this article, the authors examined the possibilities of using the existing GNSS infrastructure to detect seismic events. For this purpose, an algorithm of automatic discontinuity detection in time series "Switching Edge Detector" was used. The reference data were the results of GNSS measurements from the integrated system (seismic / GNSS / PSInSAR) installed on the LGCB (Legnica-Głogów Copper Belt) area. The GNSS data from 2020 was examined, for which the integrated system registered seven seismic events. The switching Edge Detector algorithm proved to be an efficient tool in seismic event detection.

Keywords: GNSS; seismology; switching edge detection; timeseries analysis

[1] UNIVERSITY OF WARMIA AND MAZURY IN OLSZTYN, FACULTY OF GEOENGINEERING, INSTITUTE OF GEODESY AND CIVIL ENGINEERING, 2 OCZAPOWSKIEGO STR., OLSZTYN, 10-900, POLAND

[2] KGHM CUPRUM SP. Z.O.O. RESEARCH AND DEVELOPMENT CENTRE, GEN. W. SIKORSKIEGO STREET 2-8, WROCŁAW, 53-659, POLAND

[3] UNIVERSITY OF WARMIA AND MAZURY IN OLSZTYN, FACULTY OF TECHNICAL SCIENCES, CHAIR OF MECHATRONICS, 2 OCZAPOWSKIEGO STR., OLSZTYN, 10-900, POLAND

* Corresponding author: dariusz.tomaszewski@uwm.edu.pl

1. Introduction

The study of the deformation of mining areas is one of the crucial elements of excavation exploitation. Grioli et al. [13] provides a comprehensive review of induced seismicity. The research conducted in this field allows determining the range of the mine's influence on the surrounding areas. It also helps by determining the damage that may occur during further mining operations. Therefore, modern mining needs information about spatio-temporal deformation processes developing in rock mass due to its activity. As a result, of deformation processes caused by changes in static stresses in the rock mass, a rapid displacement, cracking, or refraction of rock layers may occur. It is called a seismic event which has a tremendous impact on the surrounding natural environment and surface structure.

Contemporary science uses many tools to detect and monitor deformations and seismic events. Depending on the needs, these tools allow the detection of desired quantities both in real-time and in the subsequent measurement data processing. A viral method of studying large land surfaces' deformation is Synthetic Aperture Radar Interferometry (InSAR). The first use of this method for such a purpose was presented by Massenet et al. in [12]. Over the years, various InSAR technology types were used to monitor and model terrain deformation regarding mining activity. Examples of Differential Synthetic Aperture Radar Interferometry (DInSAR) use include monitoring 15 years of operation of a coal mine in France [43] or mapping ground movements in open pit iron mines near the Amazon river [16]. Similar studies were performed for significant deformation mining subsidence in China [17]. Further examples of likewise studies were carried out in Europe to monitor active and abandoned coal mines [29,32,41]. In the presented cases, the accuracy of the method varied within a few millimetres. Despite the high accuracy and the possibility of obtaining data on large areas, InSAR methods have their limitations. One of the most critical limitations of this method is the continuity of the data. Currently used satellites Sentinel-1A and Sentinel-1B have a six-day repeat cycle, which means that one will receive the data to be processed once every six days [11]. In connection to the above, the InSAR methods allow for very high accuracy, but it is not possible to use them for kinematic monitoring. They are perfect for studying long-term deformation of the terrain but inappropriate for detecting a single seismic event. InSAR will allow seeing the influence of mining activity on the terrain surface, but it will not determine the exact size of a single seismic event. The only information regarding the time of a seismic event will be that it took place between one image and the next one. Modern mine operation requires information regarding land deformation and quick response to seismic events, epicentre detection, determination of the range and prediction of its consequences. Therefore, other methods are used for this type of task. In every place, the seismic activity will be monitored by geological services using networks of seismometers [3,28,30,44,]. They allow for the detection simultaneously of the shock and the location of the epicentre. But, they will not show the deformation of the earth's crust caused by a tremor. Another method that allows for measurements in a global reference system is Global Navigation Satellite Systems (GNSS) satellite measurement systems. For this purpose, networks of permanent GNSS stations are set up to monitor land deformation in near real-time [36,45]. These methods allow for both long-term deformation monitoring and detection of seismic events. Examples of deformation studies using GNSS technology are presented worldwide, such as the biggest nickel production base in China – the Jinchuan mine [14]. Combined GNSS and Permanent Scatterers Synthetic Aperture Radar Interferometry (PSInSAR) monitoring were used in Australia [2,5,25]. Also, contemporary research shows that a high rate of GNSS can be used to study both the amplitude and frequency

of seismic events [21]. As can be seen, modern geodesy has created various tools that allow the study of mine areas and predict the consequences of mining activity on the surrounding environment. In the areas that are particularly exposed to damage related to mining activities, a network of seismometers and GNSS stations are created along with InSAR data development. It provides complete information considering deformation and seismic events. However, it is not applicable in all mining areas. Therefore, researchers often use existing infrastructure for this purpose. For example, it is possible to study seismic events based on the analysis of results from the existing networks of GNSS reference stations (EUREF permanent network, IGS stations, and local GNSS augmentation systems) [3,45]. Such a solution allows for active monitoring of a given area and the detection of previous seismic events based on the archival data of the station. Permanent GNSS receiver networks are now very developed and widespread. They provide information on position, deformation, coordinate system definitions, time, and space weather. Network density is very high and consists of both national and commercial networks. GNSS receivers are evenly distributed throughout Poland. The key issue in the operation of these networks is the knowledge of the correct and unchanging position of GNSS antennas, which affects all parameters determined by these stations. Many regions with reference stations are subject to seismic activity due to the ongoing mining exploitation. Seismic activity may or may not cause terrain deformation and displacement of the antenna at one of the network points. Therefore, it is crucial to determine whether the shock has occurred and whether it has displaced the receiver antenna. If the displacement of the receiver antenna is detected, it is necessary to calculate and correct the coordinates of the GNSS stations. At the same time, the even distribution of reference stations may allow the detection of the amount of deformation that occurred from seismic activity. The analyses from the results of time-series can also be redundant and partial validation of data from accelerometers. An important aspect here is the determination of the magnitude of the terrain displacement caused by the seismic event.

Detection of seismic events can be done by analysing the time series from the GNSS station located in the studied area. However, without additional information (e.g., from a seismometer network), finding a seismic event is a problematic task. The task will come down to finding discontinuities of data and determining the size of the found change. Researchers can have an event date list and, on its basis, check whether the area where a given station is located has been deformed at a given time [7]. One can also view the time series of positioning results from reference stations and manually identify the discontinuity based on height diagrams [24]. However, these are time-consuming and inefficient methods in the case of multiple stations. Therefore, there is a group of automatic methods used for time series analysis and discontinuities detection. The use of variational models for signal segmentation was presented in [1]. Also, the use of wavelets and Bayesian methods is presented similarly in this publication [1]. These methods worked very well, but they have not determined the magnitude of the event, only its occurrence. In [33], the Detection Identification Adaptation (DIA) procedure was applied to the coordinate time-series. An overview of available methods can be found in [19], where the authors point out that further research and development of both automatic and manual methods is necessary. Promising research has been done to find the optimal strategy for time series discontinuity detection to estimate vertical crustal movements [22,23]. In these studies, an algorithm based on the switching edge detector was used. It allowed the detection of discontinuities and then determining the size of detected data "jumps".

This article aims to present the use of the SED (Switching Edge Detector) algorithm to detect seismic events resulting from mining operations. The main goal of this paper is to test this

methodology through a case study located in LGCB [28]. The research was carried out based on data from the system that integrates seismometers, GNSS stations, and PSinSAR, established in the vicinity of the Rudna Copper mine in Poland. This mine is a part of the Legnica – Głogów Copper Belt (LGCB) area. The exploited deposit of copper is located in the Fore-Sudetic Monocline in the South-West part of Poland. The deposit is located at a depth of 300 m to 1300 m with a 6º dip towards the NS, and it has a thickness ranging from 0.4 m to 18.0 m. This area is one of the most seismically active in Europe [18,26,27]. The application of GNSS measurements to evaluate tremors and terrain deformations in this area can be found in many scientific publications [21,45]. The use of an integrated Seismic/GNSS/PSinSAR system as a reference to GNSS data allowed to check whether the presented algorithm detects actual seismic events.

2. Switching Edge Detector

Switching Edge Detector was used to detect seismic events in the GNSS station position time series. This algorithm was presented by D. Smith in 1998 [8]. The former tests to detect discontinuities in data from reference stations showed that the algorithm is susceptible to outliers [22]. Therefore, in the presented method of detecting seismic events, two-stage processing of observational data was used. The original assumption of the SED algorithm was enhanced with a mechanism for detecting and removing outliers. Many methods of detecting outliers exist in the literature. The earliest algorithms assume a statistical approach. These methods most often involve the analysis of one-dimensional data [35,40]. However, they are also used in multi-variant data sets [20]. Unfortunately, the problem of numerous dimensions of the tested samples significantly prolongs finding and eliminating outliers. This phenomenon is known as the "Curse of Dimensionality" [9,34]. In statistical methods, researchers use proximity-based techniques [31], parametric methods [35], non-parametric methods [10], semi-parametric methods [38]. In addition to statistical methods, one can use supervised [4,6] or unsupervised neural networks [39]. Researchers also use machine learning and some hybrid systems to detect outliers [4,6]. In the case of GNSS time-series, authors dealt with one-dimension that statistical tests can easily process. The tested data has one dimension because each of the analysed coordinates for each station was processed as an independent source of information. The Grubbs' test was chosen to detect outliers because it had previously shown excellent results with this type of data [15,22,23,42]. The final seismic event detection algorithm is comprised in Fig. 1.

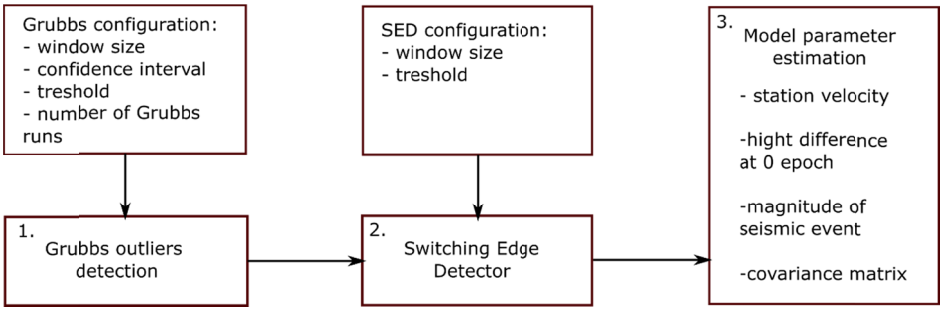

Fig. 1. Schema of seismic events detection algorithm

The Grubbs test was designed to test the null hypothesis H0 – there are no outliers in the data set and an alternative hypothesis Ha – there is exactly one outlier in the data set. Therefore, a single analysis with the Grubbs test makes it possible to find a maximum of one outlier. The statistical Grubbs test is defined as:

$$G = \frac{\max \left| Y_i - \underline{Y} \right|}{s} \tag{1}$$

Where: Y_i – current sample (in case of these data, window sample), $\underline{Y}$ – mean value, s – standard deviation.

The limitation of the Grubbs test is that it cannot be used for large data sets. Research has shown that it works best for sets not exceeding 25 samples. Since in the case of GNSS station's time series, the data sets are much larger, a moving window was used inside which the Grubbs test was performed. Each window ranged from $n - i$ ton $n + i$ where i denotes the $i - th$ observation and n represents half the window size for the Grubbs test. In a single Grubbs test, the p-value is understood as a chance of a certain point being so far from other points. Qualifying a point as an outlier is performed based on the rank of that point. If a point was defined as the outlier (in a single Grubbs test), then the probability of this point being an outlier was defined as 1 and the rank of the point rose by 1. Next, i increased by 1, and the test was conducted again. After testing the entire set, the algorithm removes the given points if their rank exceeds the predefined threshold. For example, if the threshold was set to 3, the point would be removed from the set when after 25 steps (window size) of Grubb's algorithm at least three times it was detected as an outlier. In the case of investigated datasets, this threshold was set to 2. After detecting an outlier, the test may remove it or replace it with an observation representing the average of the neighbouring values. Due to the size of the analysed sets, the choice of one of these two solutions is not statistically significant. Therefore, outliers were removed.

After removing outliers, the next step is the detection of seismic events using the Switching Edge Detector [30]. This algorithm assumes that each time series distribution is consistent with the idea of the Gaussian random process. The first step is to construct moving averages $H_{i\pm}$ as:

$$H_{i\pm} = \frac{1}{n}\sum_{k=1}^{n} h_{i\pm k} \tag{2}$$

Where point h is defined at time i in $n - point$ window.

Then, on the basis of the obtained averages, moving variances are constructed.

$$S_{i\pm} = \frac{1}{n}\sum_{k=1}^{n} \left(h_{i\pm k} - H_{i\pm} \right)^2 \tag{3}$$

Ideally, the output function would be as follows:

$$H_{out}\left(i\right) = \frac{H_{i+} - H_{i-}}{S_i} \tag{4}$$

where S_i is the variance of the noise estimated from one window. In practice, the edge location (seismic event) is unknown, so Chung and Kennedy [37] proposed using variance to calculate the switching factors g_{i+}, g_{i-}.

$$g_{i+} = \frac{S_{i-}^{2r}}{S_{i+}^{2r} + S_{i-}^{2r}},\ g_{i-} = \frac{S_{i+}^{2r}}{S_{i+}^{2r} + S_{i-}^{2r}} \tag{5}$$

where r is an arbitrary selected exponent with a value $r \gg 1$. Then the output function is as follows:

$$H_{out}(i) = g_{i+} H_{i+} + g_{i-} H_{i-} \tag{6}$$

The result of the SED algorithm is the matrix C containing zeros and ones. This matrix describes at which epoch an edge was detected. The number of columns in this matrix corresponds to the number of epochs in studied data, and the number of rows corresponds to the number of seismic events (edges) found. Each row has zeros up to the point where an edge is detected. After an edge is detected, the zeros change to ones. The mathematical model used in detection is a straight line described by the following function [30]:

$$h(t) = vt + h_0 + c_1 s_1 + c_2 s_2 + \ldots + c_m s_m \tag{7}$$

where: t – epoch, $h(t)$ – height difference in epoch t, v – velocity between GNSS stations, h_0 – height difference in epoch t_0, $c_1, c_2, \ldots, c_m$ – elements of matrix C and $s_1, s_2, \ldots, s_m$ – magnitude of the "events"":'

For n number of points, in the matrix notation:

$$L = \left[A : C^T \right] X$$

where:

$$L = \left[h(t_1) h(t_2) \vdots h(t_n) \right],\ X = \left[v\, h_0\ \ s_1\, s_2 \vdots s_m \right],\ A = \left[t_1\, t_2 \vdots t_n 1 1 \vdots 1 \right],$$
$$C^T = \left[c_{[1,1]}\, c_{[1,2]} \cdots c_{[1,m]}\, c_{[1,2]}\, c_{[2,2]} \cdots c_{[2,m]} \vdots c_{[n,1]}\, c_{[n,2]} \cdots c_{[n,m]} \right] \tag{8}$$

This model can be fitted using Least Squares (LS) adjustment. Ultimately, the form of the C matrix allows the detection and marking of seismic events (Fig. 2).

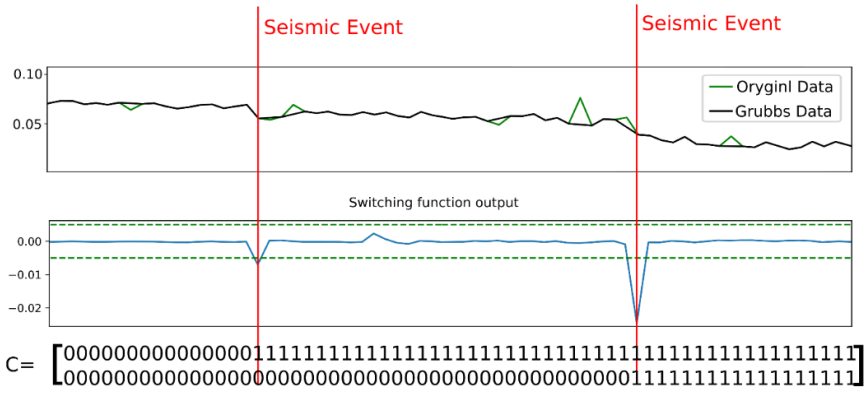

Fig. 2. An example of joint Grubbs and SED algorithms operation

Experiment Data

The data selected for the experiment comes from the paraseismic monitoring system installed near the copper mine in Polkowice, Poland. This mine is a part of the LGCB (Legnica-Głogów COPPER Belt) area and is located in the Southern-West region of Poland. The deposit is located at a depth of 300 to 1300 metres and a thickness of 0.4 to 18 m. To properly monitor the seismic activity in the mine area, a system has been installed using accelerometer measurements, PSInSAR imaging analysis, and a network of GNSS stations. The system has been designed so that it is possible to immediately detect a seismic event and then determine the impact of this event on the environment. The system consists of 10 seismic stations (Fig. 3) and 10 GNSS stations, of which four are used as reference stations (PRAC, GAWO, GREB, CUPR) and are located outside the mine's influence area (Fig. 5). The distribution of the seismic stations mostly coincides with the location of the GNSS stations. In addition to the PSInSAR system, eight pairs of Artificial Corner Reflectors (ACR) were built (Fig. 4, depicted as red triangles). Corner reflectors

Fig. 3. Placement of seismometer stations near Polkowice copper mine

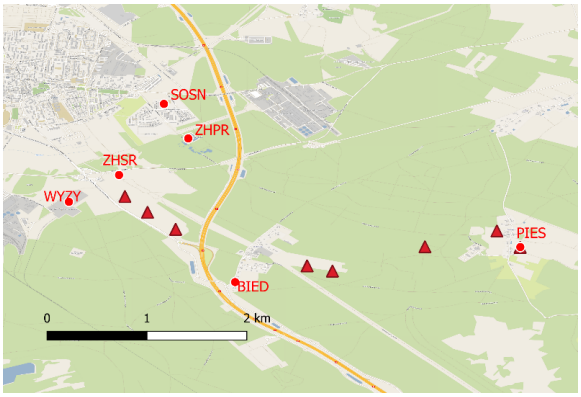

Fig. 4. Placement of Artificial Corner Reflectors (ACR) near Polkowice copper mine

are placed above the mining activity area in places where natural scatterers were observed. The accelerometers at SGOR, TARN, JEDR and ZGLU stations are not collocated with the GNSS stations because seismic stations are placed directly above the mine influence area.

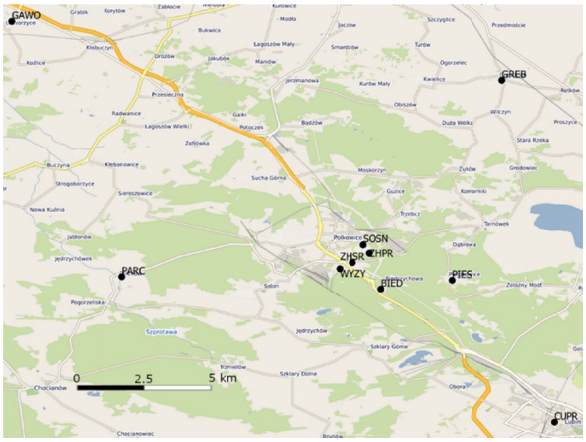

Fig. 5. Placement of GNSS stations near Polkowice copper mine

To test the SED algorithm, the time-series of GNSS processing results from 2020 have been used. GNSS time series were calculated as daily double differenced multi-station solutions with GAWO, GREB, CUPR and PRAC as reference stations (using Bernese software). At that time, the integrated system recorded seven seismic events that resulted from the exploitation of the copper mine, and their epicentres were located in the studied area (Table 1). Two of them were characterised by the greatest energy. The first was recorded on July 22, 2020, at 03:46 pm UTC near the PIES station, with a power of En = 1.9×108 J (M = 3.6). The second one with the power En = 1.1×107 (M = 3.0) took place on July 30, 2020, near the WYZY station at 5:36 pm UTC. The first event is an order of magnitude larger than the second one and belongs to the phenomena distant from the front and occurring in the zones of larger faults separating the mining plots. This type of tremor occurs less frequently and can be registered once a year on average. The second

TABLE 1

List of seismic events near the tested area, during the year 2020

Nr.	Date	DoY	Hour. (UTC + 2h)	Energy [J]	Magnitude
1	2	3	4	5	6
1	2020-02-13	44	17:51	1,4E+06	2,5
2	2020-04-05	95	08:02	1,1E+06	2,6
3	2020-04-24	114	07:30	1,0E+06	2,5
4	2020-05-08	128	05:48	2,1E+06	2,6
5	2020-07-03	184	23:50	1,1E+06	2,5
6	2020-07-22	203	03:46	1,9E+08	3,6
7	2020-07-30	211	17:36	1,1E+07	3,0

one belongs to the group of earthquakes that occur in the vicinity of the exploitation front and is one of the most frequent seismic phenomena.

Based on seismometer readings, the location of the epicentres of the detected events was determined (Fig. 6).

Fig. 6. Location of epicentres of tested seismic events

All epicentres were marked as orange stars. As it can be noticed, considered seismic events were located near GNSS stations, which is visible in these stations' results. It is also the basis for the tests of the SED automatic detection of these events. Four events took place in the vicinity of WYZY. The following three events had their epicentres close to the PIES station. The time series from these three stations were analysed with the developed algorithm. The y, x, and h coordinates in the East-North-Up (ENU) reference system were interpreted. The analyses were performed for the x (N), y (E), and h (U) coordinates because the sequences of seismic events are visible both at the height and rectangular coordinates. Due to the higher accuracy of the x, and y coordinates, other parameters of the algorithm were used to analyse these series (Table 2).

TABLE 2

SED and Grubbs algorithms settings

	x, y coordinates	**Height h component**
Data sampling	**One day**	
SED threshold	0,003 [m]	0,005 [m]
SED Window	20	20
Grubbs Window	30	20
Grubbs threshold	2 alpha	2 alpha
Number of Grubbs tests	1	1

The graphs (Figs 7-9) show the results of the SED analyses for the GNSS station's coordinates time series. In each of the figures, the results are presented by four graphs that show the results of the successive stages of the SED algorithm. In all graphs, the values presented on the horizontal axis correspond to the Day of Year (DoY) number. The top graph corresponds to the values of left and right moving averages calculated based on equation (2). The second graph depicts the standard deviations of the moving averages, which shows the variability of the set.

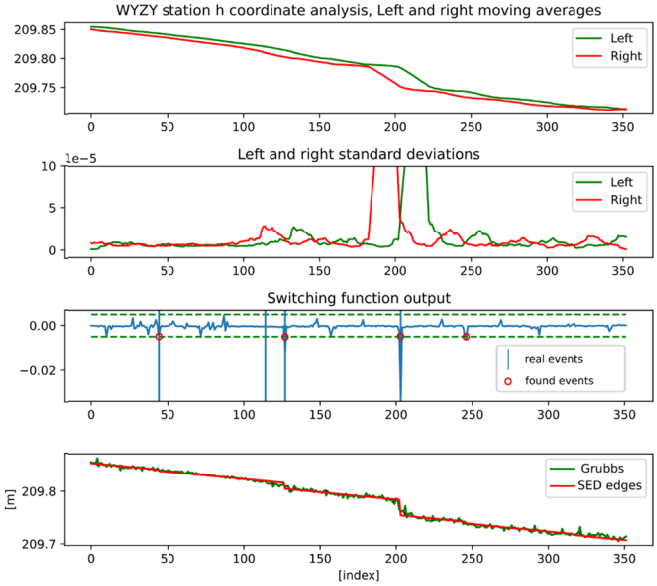

Fig. 7. WYZY station h coordinate analysis

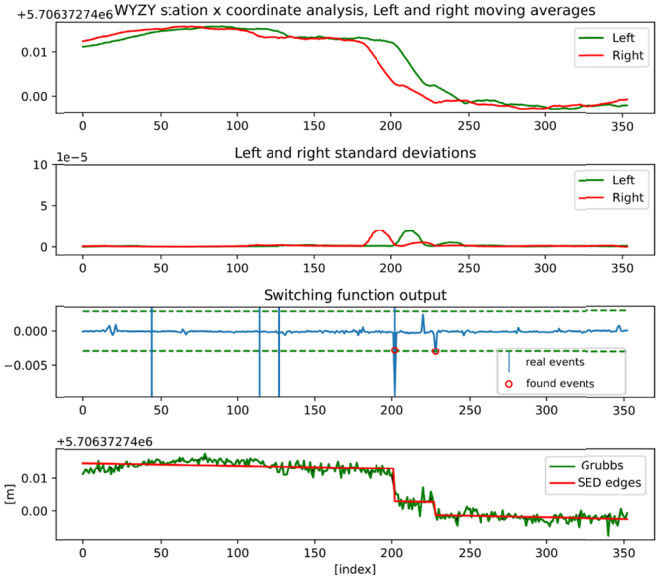

Fig. 8. WYZY station x coordinate analysis

Found seismic events can be best seen on the “switching output function” chart. These graphs depict where the SED output values exceeded the assumed threshold (marked with a green dashed line). Additionally, in the same chart, the actual occurrences of seismic events are marked with

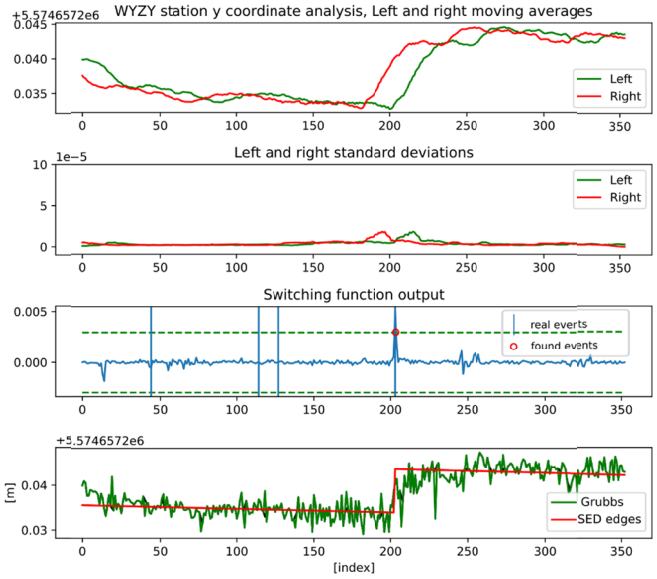

Fig. 9. WYZY station y coordinate analysis

blue lines. The fourth graph depicts the analysed data, making it possible to check whether the found "jumps" are visible in the time series.

Near the WYZY station, four seismic events could have influenced the subsoil's deformation located under the station. These events occurred on 2/13 (DoY 44), 4/24 (DoY 144), 5/8 (DoY 128), and 7/22 (DoY 203). The analysis of changes in the WYZY station's altitude made it possible to detect three seismic events during this time (DoY 44, 128, 203). The event from DoY 114 was not detected. However, one should note that this is a lower energy event and is not visible in the observation result. The analysis of the rectangular plane coordinates (x, y) confirms the detection of the event from day 203. It is the event of the highest energy and magnitude in this region, so it caused deformations in all studied directions. The rest of the events are not visible in the x, y coordinate series. At the same time, an edge on day 228 was detected at the x-coordinate and is reflected in the observation results. The coordinate analysis shows that there was also a rapid change in the positioning results on that day, but in the following days, the previous value returned. This shift is not a consequence of a seismic event because other systems did not detect it. However, it cannot be treated as an algorithm error because the detected "jump" is visible in the coordinate time series.

Three epicentres were located near the PIES station (Figs 10-12). Considered events occurred on 4/5 (DoY 95), 3/7 (DoY 184), and 30/7 (DoY 211). However, the analysis of the time series showed different results than in the case of WYZY stations. Seismic events from days 95 and 184, as those characterised by lower energy, were not detected. They are not visible in the time series from the station under study. The SED algorithm detected the event of DoY 211, somehow with one of the highest energy and magnitude in all three investigated directions (x, y, h). Additionally, the altitude analysis allowed the detection of seismic events from DoY 44 and 128, even though their epicentres were not located in the vicinity of the PIES station. Analysis of the x coordinate

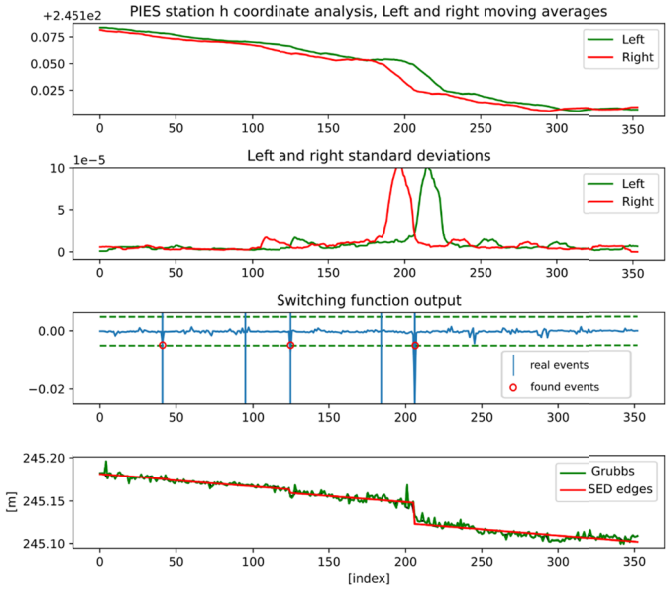

Fig. 10. PIES station h coordinate analysis

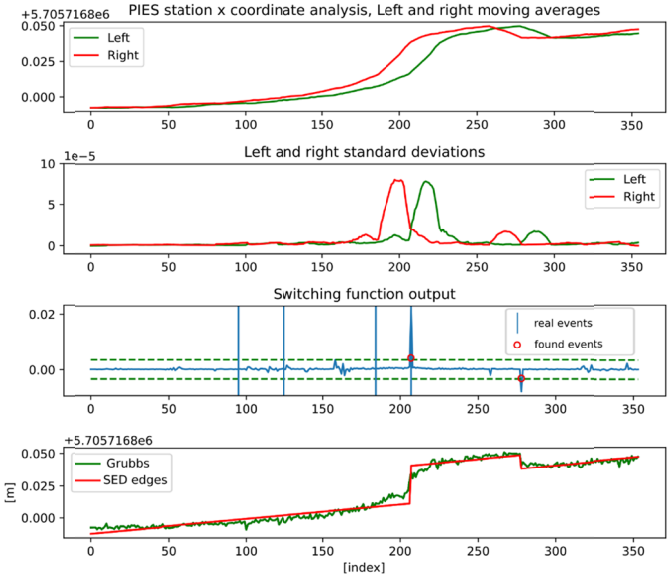

Fig. 11. PIES station x coordinate analysis

also detected the event on day 44. On both rectangular coordinates, the SED algorithm detected a “jump” on day 278 and is visible in the time series from the PIES station. Other systems did not detect this deformation. However, it cannot be treated as a malfunction of the algorithm.

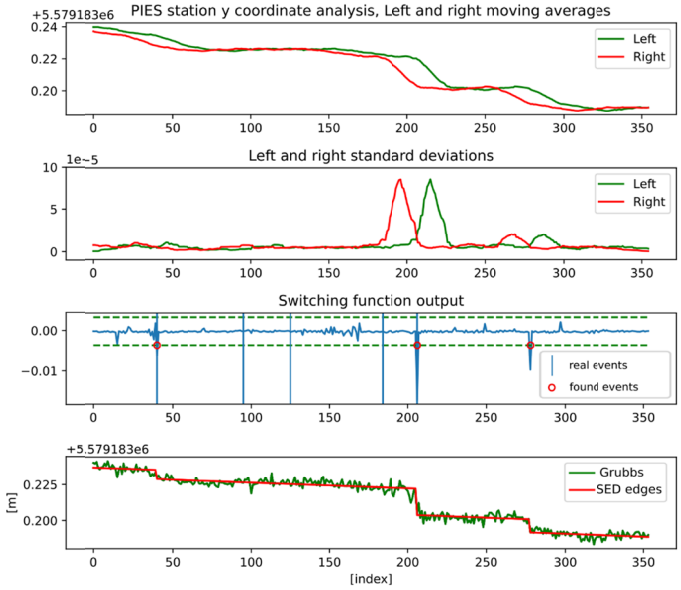

Fig. 12. PIES station y coordinate analysis

The same analyses were performed for all GNSS stations in the study area. The results of these studies are presented in Table 3.

TABLE 3

List of detected seismic events at individual GNSS stations

Station name	DoY of seismic event						
	44	95	114	128	184	203	211
WYZY	■			■		■	
PIES	■			■			■
BIED				■	■		
ZHPR				■		■	
SOSN				■		■	
ZHSR				■		■	

In addition to the detected session events at the ZHPR and SOSN stations, a “jump” was also detected on day 246, analogical as in the WYZY station analysis. The reason for such a situation was the malfunction of the receiver on the ZHPR station. The receiver stopped working for 2 weeks, which introduced changes in the daily adjustment results. These changes were detected as a jump by the SED algorithm.

3. Conclusions

Our research analyses the performance of the “Switching Edge Detector” algorithm. It was applied to the GNSS positioning time series in the copper mine exploration area. This study aimed

at checking whether it is possible to automatically detect seismic events based on the analysis of the time series with the proposed algorithm. All three components of the position were analysed, assuming various parameters for height and rectangular coordinates. Based on data analysis from 7 stations, 5 out of 7 seismic events in the studied area in 2020 were detected. Undetected events (DoY 95 and 114) were characterised by the lowest energy and were not visible in time series. Some of the events have been detected multiple times. An example is an event of DoY 128, which was detected while analysing all GNSS stations. Although this event's epicentre was near the WYZY station, it is visible in the PIES station's time series 5 km away. A similar situation can be observed for the event of DoY 203, which was detected after analysing the results from 4 GNSS stations. The highest energy characterises the second event in the analysed period. Therefore, at three stations, it was detected for all studied directions. Additionally, in 5 cases, the algorithm detected one event that was not registered by the seismometers. This was caused by the malfunction of the GNSS receiver at the ZHPR station.

The tested algorithm allowed for the detection of 70% of seismic events recorded by other devices. The events that were not detected did not cause deformation of the ground that would affect the positioning results, so they are not visible in the time series. All detected events had energies above 1.1E + 06 J, which suggests that lower energy events have too little influence on the positioning results to be automatically detected. The remaining "jumps" in the data detected by the algorithm cannot be treated as a malfunction because there are indications that there have been real changes in the GNSS stations' position these days. These changes may have resulted from the seismic or non-seismic activity.

Acknowledgments

This document is the results of the research project funded by the Project No. POIR.04.01.04-00-0056/17/The European Regional Development Fund within the Smart Growth Operational Programme 2014-2020.

References

[1] A. Borghi, L. Cannizzaro, A. Vitti, Advanced techniques for discontinuity detection in GNSS coordinate time-series. An Italian case study. Geodesy for Planet Earth, 627-634 (2012). DOI: https://doi.org/10.1007/978-3-642-20338-1_77

[2] A.H.M. Ng, L. Ge, K. Zhang, H.C. Chang, X. Li, C. Rizos, M. Omura, Deformation mapping in three dimensions for underground mining using InSAR-Southern highland coalfield in New South Wales, Australia. International Journal of Remote Sensing **32** (22), 7227-7256 (2011). DOI: https://doi.org/10.1080/01431161.2010.519741

[3] A. Leśniak, Z. Isakow, Space-time clustering of seismic events and hazard assessment in the Zabrze-Bielszowice coal mine, Poland. International Journal of Rock Mechanics and Mining Sciences **46** (5), 918-928 (2009). DOI: https://doi.org/10.1016/j.ijrmms.2008.12.003

[4] A. Nairac, N. Townsend, R. Carr, S. King, P. Cowley, L. Tarassenko, A system for the analysis of jet engine vibration data. Integrated Computer-Aided Engineering **6** (1), 53-66 (1999). DOI: https://doi.org/10.5555/1275794.1275800

[5] B. Antonielli, A. Sciortino, S. Scancella, F. Bozzano, P. Mazzanti. Tracking Deformation Processes at the Legnica Glogow Copper District (Poland) by Satellite InSAR – I: Room and Pillar Mine District. Land **10** (6), 653 (2021). DOI: https://doi.org/10.3390/land10060653

[6] C.M. Bishop, Novelty detection and neural network validation. IEEE Proceedings-Vision, Image and Signal Processing **141** (4), 217-222 (1994). DOI: https://doi.org/10.1049/ip-vis:19941330

[7] C. Volksen, J. Wassermann, Recent crustal deformation and seismicity in Southern Bavaria revealed by GNSS observations. Proceedings of the EUREF Symposium. 29-31 (2013).

[8] D.A. Smith, A quantitative method for the detection of edges in noisy time–series. Philosophical Transactions of the Royal Society of London. Series B: Biological Sciences **353** (1378), 1969-1981 (1998). DOI: https://doi.org/10.1098/rstb.1998.0348

[9] D.B. Skalak, Prototype and feature selection by sampling and random mutation hill climbing algorithms. Machine Learning Proceedings 293-301 (1994). DOI: https://doi.org/10.5555/3091574.3091610

[10] D. Dasgupta, S. Forrest, Novelty detection in time series data using ideas from immunology. Proceedings of the international conference on intelligent systems 82-87 (1996).

[11] D. Geudtner, R. Torres, P. Snoeij, M. Davidson, B. Rommen, Sentinel-1 System capabilities and applications. IEEE Geoscience and Remote Sensing Symposium 1457-1460 (2014). DOI: https://doi.org/10.1109/IGARSS.2014.6946711

[12] D. Massonnet, M. Rossi, C. Carmona et al. The displacement field of the Landers earthquake mapped by radar interferometry. Nature. **364**, 138-142 (1993). DOI: https://doi.org/10.1038/364138a0

[13] F. Grigoli, S. Cesca, E. Priolo, A.P. Rinaldi, J.F. Clinton, T.A. Stabile, B. Dost, M. Garcia Fernandez, S. Wiemer, T. Dham, Current challenges in monitoring, discrimination and management of induced seismicity related to underground industrial activities: a European perspective. Reviews of Geophysics **55** (4), (2017). DOI: https://doi.org/10.1002/2016RG000542

[14] F. Ma, H. Zhao, Y. Zhang, J. Guo, A. Wei, Z. Wu, Y. Zhang, GPS monitoring and analysis of ground movement and deformation induced by transition from open-pit to underground mining. Journal of Rock Mechanics and Geotechnical Engineering **4** (1), 82-87 (2012). DOI: https://doi.org/10.3724/SP.J.1235.2012.00082

[15] F.E. Grubbs, Procedures for detecting outlying observations in Samples. Technometrics **11**, 1-21 (1969). DOI: http://dx.doi.org/10.1080/00401706.1969.10490657

[16] G. Herrera, R. Tomás, F. Vicente, J.M. Lopez-Sanchez, J.J. Mallorquí, J. Mulas, Mapping ground movements in open pit mining areas using differential SAR interferometry. International Journal of Rock Mechanics and Mining Sciences **47** (7), 1114-1125 (2010). DOI: https://doi.org/10.1016/j.ijrmms.2010.07.006

[17] H.D. Fan, G. Wei, Q. Yong, J.Q. Xue, B.Q. Chen, A model for extracting large deformation mining subsidence using D-InSAR technique and probability integral method. Transactions of Nonferrous Metals Society of China **24** (4), 1242-1247 (2014). DOI: https://doi.org/10.1016/S1003-6326(14)63185-X

[18] I. Kudłacik, J. Kapłon, G. Lizurek, M. Crespi, G. Kurpiński. High-rate GPS positioning for tracing anthropogenic seismic activity: The 29 January 2019 mining tremor in Legnica-Głogów Copper District, Poland. Measurement 168 (2021). DOI: https://doi.org/10.1016/j.measurement.2020.108396

[19] J. Gazeaux, S. Williams, M. King, M. Bos, R. Dach, M. Deo, F.N. Teferle, Detecting offsets in GPS time series: First results from the detection of offsets in GPS experiment. Journal of Geophysical Research: Solid Earth **118** (5), 2397-2407 (2013). DOI: https://doi.org/10.1002/jgrb.50152

[20] J. Laurikkala, M. Juhola, E. Kentala, N. Lavrac, S. Miksch, B. Kavsek, Informal identification of outliers in medical data. Intelligent data analysis in medicine and pharmacology **1**, 20-24 (2000).

[21] J. Paziewski, G. Kurpinski, P. Wielgosz, L. Stolecki, R. Sieradzki, M. Seta, F. Martin-Porqueras, Towards Galileo+ GPS seismology: Validation of high-rate GNSS-based system for seismic events characterisation. Measurement **166**, 108236 (2020). DOI: https://doi.org/10.1016/j.measurement.2020.108236

[22] J. Rapiński, K. Kowalczyk, Detection of discontinuities in the height component of GNSS time series. Acta Geodynamica et Geomaterialia **13** (3), 315-320 (2016). DOI: https://doi.org/10.13168/AGG.2016.0013

[23] K. Kowalczyk, J. Rapiński, Verification of a GNSS Time Series Discontinuity Detection Approach in Support of the Estimation of Vertical Crustal Movements. ISPRS Int. J. Geo-Inf. **7**, 149 (2018). DOI: https://doi.org/10.3390/ijgi7040149

[24] K. Tretyak, S. Dosyn, Study of vertical movements of the European crust using tide gauge and GNSS observations. Reports on Geodesy and Geoinformatics **97** (1), 112-131 (2015). DOI: https://doi.org/10.2478/rgg-2014-0016

[25] L. Ge, C. Rizos, S. Han, H. Zebker, Mining subsidence monitoring using the combined InSAR and GPS approach. Proceedings of the 10th International Symposium on Deformation Measurements. 1-10 (2001).

[26] L. Stolecki, Badania rozkładów parametrów drgań generowanych wstrząsami górniczymi w kopalniach LGOM. CUPRUM Czasopismo Naukowo-Techniczne Górnictwa Ród **3** (60), 29-37 (2011).

[27] L. Stolecki, W. Grzebyk, The velocity of roof deflection as an indicator of underground workings stability – Case study from polish deep copper mines. International Journal of Rock Mechanics and Mining Sciences **143** (2021).

[28] Ł. Rudziński, S. Lasocki, B. Orlecka-Sikora, J. Wiszniowski, D. Olszewska, J. Kokowski, J. Mirek, Integrating Data under the European Plate Observing System from the Regional and Selected Local Seismic Networks in Poland. Seismological Research Letters **92** (3), 1717-1725 (2021). DOI: https://doi.org/10.1785/0220200354

[29] M.C. Cuenca, A.J. Hooper, R.F. Hanssen, Surface deformation induced by water influx in the abandoned coal mines in Limburg, The Netherlands observed by satellite radar interferometry. Journal of Applied Geophysics **88**, 1-11 (2013). DOI: https://doi.org/10.1016/j.jappgeo.2012.10.003

[30] M.D.G. Salamon, G.A. Wiebols, Digital location of seismic events by an underground network of seismometers using the arrival times of compressional waves. Rock Mechanics **6** (3), 141-166 (1974). DOI: https://doi.org/10.1007/BF01238422

[31] M. Ester, H.P. Kriegel, J. Sander, X. Xu, A density-based algorithm for discovering clusters in large spatial databases with noise. Kdd. **96**, 226-231 (1996). DOI: https://doi.org/10.5555/3001460.3001507

[32] M. Ilieva, P. Polanin, A. Borkowski, P. Gruchlik, K. Smolak, A. Kowalski, W. Rohm, Mining deformation life cycle in the light of InSAR and deformation models. Remote Sensing **11** (7), 745 (2019). DOI: https://doi.org/10.3390/rs11070745

[33] N. Perfetti, Detection of station coordinate discontinuities within the Italian GPS Fiducial Network. Journal of Geodesy **80** (7), 381-396 (2006). DOI: https://doi.org/10.1007/s00190-006-0080-6

[34] P. Datta, D. Kibler, Learning prototypical concept descriptions. Machine Learning Proceedings 158-166 (1995). DOI: https://doi.org/10.1016/b978-1-55860-377-6.50028-1

[35] P.J. Rousseeuw, A.M. Leroy, Robust regression and outlier detection **589**, 2005 John Wiley & Sons.

[36] R. Baryła, J. Paziewski, P. Wielgosz, K. Stepniak, M. Krukowska, Accuracy assessment of the ground deformation monitoring with the use of GPS local network: open pit mine Koźmin case study. Acta Geodynamica et Geomaterialia **11** (4), (2014). DOI: https://doi.org/10.13168/AGG.2014.0013

[37] S.H. Chung, R.A. Kennedy, Forward-backward non-linear filtering technique for extracting small biological signals from noise. Journal of Neuroscience Methods **40** (1), 71-86 (1991). DOI: https://doi.org/10.1016/0165-0270(91)90118-j

[38] S. Roberts, L. Tarassenko, A probabilistic resource allocating network for novelty detection. Neural Computation **6** (2), 270-284 (1994). DOI: https://doi.org/10.1162/neco.1994.6.2.270

[39] T. Kohonen, Exploration of very large databases by self-organizing maps. Proceedings of international conference on neural networks **1**, (1997). DOI: https://doi.org/10.1109/ICNN.1997.611622

[40] V. Barnett, T. Lewis, Outliers in statistical data. 1984 John Wiley & Sons, Singapore. DOI: https://doi.org/10.1002/bimj.4710300725

[41] W. Milczarek, J. Blachowski, P. Grzempowski, Application of PSInSAR for assessment of surface deformations in post-mining area – case study of the former Walbrzych hard coal basin (SW Poland). Acta Geodynamica et Geomaterialia **14** (1), 41-52 (2017). DOI: https://doi.org/10.13168/AGG.2016.0026

[42] W. Stefansky, Rejecting outliers in factorial designs. Technometrics **14**, 469-479 (1972).

[43] Y. Guéguen, B. Deffontaines, B. Fruneau, M. Al Heib, M. de Michele, D. Raucoules, J. Planchenaul, Monitoring residual mining subsidence of Nord/Pas-de-Calais coal basin from differential and Persistent Scatterer Interferometry (Northern France). Journal of Applied Geophysics **69** (1), 24-34 (2009). DOI: https://doi.org/.1016/j.appgeo.2009.02.008

[44] T. Veikkolainen, J. Kortström, T. Vuorinen, I. Salmenperä, T. Luhta, P. Mäntyniemi,T. Tiira. The Finnish national seismic network: Toward fully automated analysis of low-magnitude seismic events. Seismological Research Letters **92** (3), 1581-1591 (2021).

[45] Z. Szczerbowski, J. Jura, Mining induced seismic events and surface deformations monitored by GPS permanent stations. Acta Geodynamica et Geomaterialia **12** (3), 237-248 (2015). DOI: https://doi.org/10.13168/AGG.2015.0023